STOCHASTIC, TIME DOMAIN MODELS AND PONTRYAGIN MAXIMUM PRINCIPLE FOR A TWO BODY WAVE POWER DEVICE

José J. Cândido[1] and Paulo A.P.S. Justino[1]

[1] Departamento de Energias Renováveis
INETI/LNEG
Estrada do Paço do Lumiar, 1649-038 Lisboa, Portugal
E-mail: Jose.Candido@ineti.pt
Paulo.Justino@ineti.pt

Abstract

In this study a stochastic model to describe the behaviour of an articulated system is developed. Optimal mechanical damping and spring coefficients are computed. Probability density functions are defined for the relevant parameters that characterize the device behaviour. For these parameters and for different sea state conditions the probability density functions are found and the articulated system is characterized in terms of these functions. Average values for useful power and capture width are also obtained for these sea state conditions.

Time domain models allow the computation of time series for the variables that characterize the wave power system behaviour. In this study a time domain model is also developed for the articulated wave power device. Results are obtained for regular and irregular waves.

Pontryagin Maximum Principle is presented as an algorithm for the control of the device.

Keywords: stochastic modelling, time domain modelling, Pontryagin Maximum Principle, two body device.

Nomenclature

A_{ij} = added mass hydrodynamic coefficient
$\hat{A}$ = complex wave elevation amplitude
$\hat{A}_n$ = complex random amplitude
B_{ij} = damping hydrodynamic coefficient
C_i = hydrostatic restoring coefficient for body *i*
D_L = damping coefficient of the power take-off equipment
$E\{\ \}$ = expected value of
F_{D_i} = complex amplitude for the diffraction force on body *i*
F_L = load force
HG_1, HG_2 = transfer function
H_s = significant wave height
K_L = spring coefficient of the power take-off equipment
M_i = mass of body *i*
$\overline{P}_I$ = incident power for a regular wave
$\overline{P}_u$ = average useful power
S_η = spectral density
T = time interval
T_e = wave energy period
Z_L = load impedance
g = acceleration of gravity
h = water depth
k = wave number
t = time
φ_n = random phase
η = sea surface elevation
λ_c = capture width
θ = wave direction angle
ρ = water specific mass
σ^2 = variance
$\hat{\xi}_i$ = complex amplitude displacement for body *i*
Max = maximum value
Min = minimum value
Ω = admissible control values

Superscripts

– = mean value
* = complex conjugate or optimum value

Subscripts

i, j = body index

1 Introduction

The ocean wave energy conversion has been a field of increasing research for some time. “In fact, there are over 1000 patented wave energy conversion techniques in Japan, North America, Western Europe, and the United Kingdom”, McCormick says, [1]. Usually wave energy converter performance is first assessed by analytical and numerical tools.

Assuming that the wave power system hydrodynamics has a linear behaviour, diffraction and radiation coefficients can be computed using, for example, WAMIT© or Aquadyn. If the power take-off equipment is considered to exhibit, in a first approach, a linear behaviour then overall (hydrodynamic plus mechanical) device performance can be studied for regular waves. In [2] a theory for wave power absorption by two independently oscillating bodies has already been devised. Frequency analysis has been used to study the performance of several single devices, such as Searev wave energy converter, [3], as well as the performance of arrays of devices, as in [4]. Hydrodynamic coefficients referring to two concentric surface-piercing truncated cylinders in heave motion were already computed in [5] using panel-method software.

A stochastic model has already been developed for OWC power plants [6]. This stochastic model has been used for optimization procedures of the Foz do Douro OWC plant, [7,8]. In this paper a stochastic model is derived for the articulated wave power device. Probability density functions are defined for the relevant parameters that characterize the device behaviour. Assuming that the overall system behaviour is linear and that the wave elevation for irregular waves may be regarded as a stochastic process with a Gaussian probability density function, the variables that define the system behaviour, such as, for example, displacements of the articulated system elements, will also exhibit a Gaussian probability density function. The probability density functions are obtained for these parameters and for different sea state conditions. The articulated system is characterized in terms of these functions. Average values for useful power and capture width are also obtained for these sea state conditions.

Time domain models allow the computation of time series for the variables that characterize the wave power system behaviour. Moreover, a time domain analysis holds the possibility of assuming a non-linear power take-off system, which is the most realistic scenario for the majority of wave power devices. In this study a time domain model is also developed for the articulated wave power device. A non-linear power take-off configuration, consisting of a hydraulic circuit with a high-pressure gas accumulator, a low-pressure gas accumulator and a hydraulic machine as in [9], is adopted. Results in regular wave conditions are obtained for this configuration, for different values of the number of pairs of sets piston/cylinder (driven by the relative displacement between the two articulated system elements) and the parameter relating flow rate through the hydraulic machine to pressure difference between the two accumulators. Results for this non-linear configuration for the power take-off and irregular waves are also computed and presented. Finally, these results are compared to the results obtained from the stochastic model.

Pontryaguin Maximum Principle is presented as an algorithm for the control of the device. Assuming that power take-off equipment presents a linear behaviour it is possible to see that damping control should be of the kind on-off except for singular arcs.

2 Mathematical models

Consider a wave energy device made of two coaxial axisymmetric oscillating bodies such that relative heave motion between bodies allows energy to be extracted from sea waves. For the purpose of this study it is assumed that the two bodies have linear hydrodynamic behaviour. A stochastic model is established and presented, based on the assumption that the power take-off system consists of a linear spring and a linear damper, whose forces are proportional to the relative displacement and to the relative velocity between bodies, respectively.

2.1 Stochastic model

Applying Newton's second law, the governing equations for the wave energy device may be written as

$$-M_1\omega^2\hat{\xi}_1 = (\omega^2 A_{11} - i\omega B_{11})\hat{\xi}_1 + (\omega^2 A_{12} - i\omega B_{12})\hat{\xi}_2 + F_{D_1} - \\ - C_1\hat{\xi}_1 - (K_L + i\omega D_L)(\hat{\xi}_1 - \hat{\xi}_2), \tag{1}$$

$$-M_2\omega^2\hat{\xi}_2 = (\omega^2 A_{22} - i\omega B_{22})\hat{\xi}_2 + (\omega^2 A_{21} - i\omega B_{21})\hat{\xi}_1 + F_{D_2} - \\ - C_2\hat{\xi}_2 + (K_L + i\omega D_L)(\hat{\xi}_1 - \hat{\xi}_2), \tag{2}$$

where ω is the angular frequency, $\hat{\xi}_i$ the complex amplitude displacement for body i, M_i the mass of body i, C_i the hydrostatic restoring coefficient for body i, A_{ij} and B_{ij} the added mass and damping hydrodynamic coefficients for body i when body j oscillates, F_{D_i} the complex amplitude for the diffraction force on body i, and K_L and D_L the spring and damping coefficients of the power take-off equipment.

Let us assume that the sea surface elevation is a Gaussian random variable in a time interval T.

Taking into consideration that the two oscillating bodies are axisymmetric and that their behaviour in the frequency domain can be described by eqs. (1) and (2), it is possible to find transfer functions, $HG_1(n\omega_0)$ and $HG_2(n\omega_0)$, where $\omega_0 = 2\pi/T$ and n is an integer, that relate the amplitude of the incident wave $\hat{A}_n$ to the displacement amplitude of body 1 and body 2, and write

$$\hat{\xi}_1(n\omega_0) = HG_1(n\omega_0)\hat{A}_n, \tag{3}$$

and,

$$\hat{\xi}_2(n\omega_0) = HG_2(n\omega_0)\hat{A}_n. \tag{4}$$

Thus, the vertical displacements for bodies 1 and 2 are described by

$$\xi_1(t) = \sum_{n=-\infty}^{+\infty} HG_1(n\omega_0)\hat{A}_n \exp(in\omega_0 t), \quad (5)$$

and

$$\xi_2(t) = \sum_{n=-\infty}^{+\infty} HG_2(n\omega_0)\hat{A}_n \exp(in\omega_0 t). \quad (6)$$

Note that, like for the sea surface elevation, ξ_1 and ξ_2 are also Gaussian random variables.

In the case of a sea state represented by a continuous power spectrum, the variances of ξ_1 and ξ_2 are

$$\sigma_{\xi_1}^2 = \int_{-\infty}^{+\infty} S_\eta(\omega)|HG_1(\omega)|^2 d\omega, \quad (7)$$

and

$$\sigma_{\xi_2}^2 = \int_{-\infty}^{+\infty} S_\eta(\omega)|HG_2(\omega)|^2 d\omega. \quad (8)$$

Assuming the load force, F_L, to be given by

$$F_L(t) = \pm \sum_{n=-\infty}^{+\infty} (K_L + in\omega_0 D_L)\left(\hat{\xi}_1(n\omega_0) - \hat{\xi}_2(n\omega_0)\right)\exp(in\omega_0 t), \quad (9)$$

using eqs. (8-9) and taking into account that $E\left\{\left(\hat{\xi}_1 - \hat{\xi}_2\right)_n \left(\hat{\xi}_1 - \hat{\xi}_2\right)_{n'}\right\} = 0$ for $n \neq n'$, the variance of the load force is

$$\sigma_{F_L}^2 = \sum_{n=-\infty}^{+\infty} |Z_L(n\omega_0)|^2 |HG_1(n\omega_0) - HG_2(n\omega_0)|^2 \sigma_n^2, \quad (10)$$

with $Z_L(n\omega_0) = K_L + in\omega_0 D_L$. For a continuous power spectrum this expression can be written as

$$\sigma_{F_L}^2 = \int_{-\infty}^{+\infty} S_\eta(\omega)|Z_L(\omega)|^2 |HG_1(\omega) - HG_2(\omega)|^2 d\omega. \quad (11)$$

The average useful power is

$$\overline{P}_u = D_L E\left\{\left|\dot{\xi}_1(t) - \dot{\xi}_2(t)\right|^2\right\}, \quad (12)$$

where $\dot{\xi}_i$ is the velocity of body *i* and, in the case of a sea state represented by a continuous power spectrum,

$$E\left\{\left|\dot{\xi}_1 - \dot{\xi}_2\right|^2\right\} = E\left\{\left(\dot{\xi}_1 - \dot{\xi}_2\right)\left(\dot{\xi}_1 - \dot{\xi}_2\right)^*\right\} = \\ = \int_{-\infty}^{+\infty} S_\eta(\omega)\omega^2 |HG_1(\omega) - HG_2(\omega)|^2 d\omega. \quad (13)$$

2.2 Time domain model

The governing equations for the wave energy device in the time domain take the form

$$(M_1 + A_{\infty_{11}})\ddot{\xi}_1(t) + A_{\infty_{12}}\ddot{\xi}_2(t) + \int_{-\infty}^{t} L_{11}(t-\tau)\ddot{\xi}_1(\tau)d\tau + \\ + \int_{-\infty}^{t} L_{12}(t-\tau)\ddot{\xi}_2(\tau)d\tau + C_1\xi_1(t) = f_{D_1}(t) + f_L(\xi_i, \dot{\xi}_i), \quad (14)$$

$$(M_2 + A_{\infty_{22}})\ddot{\xi}_2(t) + A_{\infty_{21}}\ddot{\xi}_1(t) + \int_{-\infty}^{t} L_{21}(t-\tau)\ddot{\xi}_1(\tau)d\tau + \\ + \int_{-\infty}^{t} L_{22}(t-\tau)\ddot{\xi}_2(\tau)d\tau + C_2\xi_2(t) = f_{D_2}(t) - f_L(\xi_i, \dot{\xi}_i), \quad (15)$$

where $\ddot{\xi}_i$ is the acceleration of body i, $A_{\infty_{ij}}$ is the limiting value, when $\omega \to \infty$, of the added mass A_{ij}, f_{D_i} the diffraction force on body *i*, and f_L the load force applied on the two bodies by the power take-off equipment, which may be a linear function of the relative velocity and/or relative displacement between bodies or a non-linear function. The convolution integrals introduced in these equations represent the memory effect in the radiation force caused by the history of the two bodies' motion ([9]). L_{ij} is a memory function, obtained from the hydrodynamic damping coefficient B_{ij} by

$$L_{ij}(t) = \frac{1}{2\pi}\int_0^\infty \frac{B_{ij}(\omega)}{\omega}\sin\omega t d\omega. \quad (16)$$

Assuming the power take-off mechanism to consist of a linear spring and a linear damper, the load force is

$$f_L(\xi_i, \dot{\xi}_i) = \pm K_L(\xi_1(t) - \xi_2(t)) \pm D_L(\dot{\xi}_1(t) - \dot{\xi}_2(t)). \quad (17)$$

The time domain analysis allows the modelling of a non-linear power take-off mechanism, which is the most realistic scenario for the majority of wave power devices. Following [9] we will consider a hydraulic circuit that includes hydraulic cylinders, high-pressure and low-pressure gas accumulators and a hydraulic motor. The relative motion between the two bodies induces the displacement of pistons inside the cylinders. A rectifying valve ensures that, whenever the bodies are moving relative to each other, the hydraulic fluid is pumped into the high-pressure accumulator and sucked from the low-pressure accumulator. The resulting pressure difference between the accumulators,, Δp_{acs}, drives the hydraulic motor, whose flow rate, q_m, is controlled according to

$$q_m(t) = (N_{pc} \cdot A_{pc})^2 G_m \Delta p_{acs}(t), \quad (18)$$

where G_m is a constant, N_{pc} the number of pairs of cylinders and A_{pc} the total effective cross-sectional area of a pair of cylinders.

Following [9], the pressure difference between the accumulators is, in turn, obtained from

$$\Delta p_{acs}(t) = \Theta_1 v_1(t)^{-\gamma} - \Theta_2 \left(\frac{V_0 - m_1 v_1(t)}{m_2} \right)^{-\gamma} . \quad (19)$$

Here, Θ_1 and Θ_2 are constants related to the assumedly isentropic processes in the high-pressure and low-pressure accumulators, respectively, $\gamma = c_p / c_v$ is the specific-heat ratio for the gas inside the accumulators, m_1 and m_2 are the masses of gas inside the high-pressure and the low-pressure accumulators, respectively, assumed to be fixed along the process, v_1 is the specific volume of gas inside the high-pressure accumulator and V_0 the total volume of gas inside the accumulators, which remains constant along the process, so that $m_1 v_1(t) + m_2 v_2(t) = V_0 = \text{constant}$ (v_2 is the specific volume of gas inside the low-pressure accumulator).

The total flow rate in the hydraulic circuit is given by the variation in the volume of gas inside the high-pressure accumulator, that is

$$q(t) - q_m(t) = -m_1 \frac{dv_1(t)}{dt}, \quad (20)$$

where q is the volume flow rate of liquid displaced by the pistons.

The useful power at a given instant, P_u, is, in any case, given by

$$P_u(t) = q_m(t) \cdot \Delta p_{acs}(t) . \quad (21)$$

2.3 Pontryagin Maximum Principle

We assuming that the PTO load force is given by

$$f_L\left(\dot{\xi}_i\right) = \pm D_L(t)\left(\dot{\xi}_1(t) - \dot{\xi}_2(t)\right), \quad (22)$$

the Pontryagin Maximum Principle (PMP) may be used to find the optimum control variable $D_L^*(t)$ that maximizes the time-averaged power production over the time interval T

$$\overline{P}_u = \frac{1}{T} \int_0^T D_L^*(t)\left(\dot{\xi}_1(t) - \dot{\xi}_2(t)\right)^2 dt. \quad (23)$$

Taking into consideration that $k_{ij}(t) = \frac{dL_{ij}(t)}{dt}$ the convolution integrals in equations (14) and (15) may be written as

$$\int_{-\infty}^{t} L_{ij}(t-\tau) \frac{d\dot{\xi}_j(\tau)}{d\tau} d\tau = \int_{-\infty}^{t} k_{ij}(t-\tau)\dot{\xi}_j(\tau) d\tau. \quad (24)$$

The state equations given by (14) and (15) may now be given by

$$\frac{d\dot{\xi}_1}{dt} = \frac{1}{A_{\infty 12}^2 - (M_1 + A_{\infty 11})(M_2 + A_{\infty 22})} \times \left((M_2 + A_{\infty 22}) \left(\begin{array}{l} \int_{-\infty}^{t} k_{11}(t-\tau)\dot{\xi}_1(\tau) d\tau + C_1\xi_1(t) + \\ \int_{-\infty}^{t} k_{12}(t-\tau)\dot{\xi}_2(\tau) d\tau - f_{D_1}(t) + D_L(t)\left(\dot{\xi}_1(t) - \dot{\xi}_2(t)\right) \end{array} \right) - A_{\infty 12} \left(\begin{array}{l} C_2\xi_2(t) - f_{D_2}(t) + \int_{-\infty}^{t} k_{21}(t-\tau)\dot{\xi}_1(\tau) d\tau + \\ + \int_{-\infty}^{t} k_{22}(t-\tau)\dot{\xi}_2(\tau) d\tau - D_L(t)\left(\dot{\xi}_1(t) - \dot{\xi}_2(t)\right) \end{array} \right) \right) \quad (25)$$

$$\frac{d\dot{\xi}_2}{dt} = \frac{1}{A_{\infty 12}^2 - (M_1 + A_{\infty 11})(M_2 + A_{\infty 22})} \times \left((M_1 + A_{\infty 11}) \left(\begin{array}{l} \int_{-\infty}^{t} k_{21}(t-\tau)\dot{\xi}_1(\tau) d\tau + C_2\xi_2(t) + \\ \int_{-\infty}^{t} k_{22}(t-\tau)\dot{\xi}_2(\tau) d\tau - f_{D_2}(t) - D_L(t)\left(\dot{\xi}_1(t) - \dot{\xi}_2(t)\right) \end{array} \right) - A_{\infty 12} \left(\begin{array}{l} C_1\xi_1(t) - f_{D_1}(t) + \int_{-\infty}^{t} k_{11}(t-\tau)\dot{\xi}_1(\tau) d\tau + \\ + \int_{-\infty}^{t} k_{12}(t-\tau)\dot{\xi}_2(\tau) d\tau + D_L(t)\left(\dot{\xi}_1(t) - \dot{\xi}_2(t)\right) \end{array} \right) \right) \quad (26)$$

$$\frac{d\xi_1}{dt} = \dot{\xi}_1 \quad (27)$$

$$\frac{d\xi_2}{dt} = \dot{\xi}_2 \quad (28)$$

Thus according to equations (25-28) the state variables are ξ_1, ξ_2, $\dot{\xi}_1$ and $\dot{\xi}_2$.

The Hamiltonian takes into consideration the state equations as well as the equation (23).

$$H = D_L(t)\left(\dot{\xi}_1(t) - \dot{\xi}_2(t)\right)^2 + \lambda_1 \frac{d\xi_1}{dt} + \lambda_2 \frac{d\xi_2}{dt} + \lambda_3 \frac{d\dot{\xi}_1}{dt} + \lambda_4 \frac{d\dot{\xi}_2}{dt}. \quad (29)$$

In order to apply PMP it is necessary to define adjoint equations that allow us to compute the adjoint variables λ_1, λ_2, λ_3 and λ_4. These equations may be obtained from the Hamiltonian relationships

$$\frac{d\lambda_1}{dt} = -\frac{\partial H}{\partial \xi_1}, \frac{d\lambda_2}{dt} = -\frac{\partial H}{\partial \xi_2}, \frac{d\lambda_3}{dt} = -\frac{\partial H}{\partial \dot{\xi}_1}, \frac{d\lambda_4}{dt} = -\frac{\partial H}{\partial \dot{\xi}_2}. \quad (30)$$

Since $H = H\left(D_L, \xi_1, \xi_2, \dot{\xi}_1, \dot{\xi}_2, \lambda_1, \lambda_2, \lambda_3, \lambda_4\right)$, then, according to PMP we must have for the optimum control variable

$$H(D_L^*,\xi_1^*,\xi_2^*,\dot{\xi}_1^*,\dot{\xi}_2^*,\lambda_1,\lambda_2,\lambda_3,\lambda_4)=$$
$$=\underset{D_L\in\Omega}{\text{Max}}\,H\left(D_L,\xi_1^*,\xi_2^*,\dot{\xi}_1^*,\dot{\xi}_2^*,\lambda_1,\lambda_2,\lambda_3,\lambda_4\right)\quad\forall t\in T \tag{31}$$

where * denotes the optimum solution and Ω is the admissible interval for the control variable D_L.

From equations (25) to (29) it may be seen that the Hamiltonian is linear in the control variable. It follows that D_L should take the Ω maximum or minimum values (except for singular arcs), and so

$$\text{If}\begin{cases}\left(\dot{\xi}_1(t)-\dot{\xi}_2(t)\right)^2+\dfrac{\lambda_3}{A_{\infty 12}^2-\left(M_1+A_{\infty 11}\right)\left(M_2+A_{\infty 22}\right)}\times\\ \times\left(\left(M_2+A_{\infty 22}\right)\left(\dot{\xi}_2(t)-\dot{\xi}_1(t)\right)+A_{\infty 12}\left(\dot{\xi}_2(t)-\dot{\xi}_1(t)\right)\right)+\\ +\dfrac{\lambda_4}{A_{\infty 12}^2-\left(M_1+A_{\infty 11}\right)\left(M_2+A_{\infty 22}\right)}\times\\ \times\left(\left(M_1+A_{\infty 11}\right)\left(\dot{\xi}_1(t)-\dot{\xi}_2(t)\right)-A_{\infty 12}\left(\dot{\xi}_2(t)-\dot{\xi}_1(t)\right)\right)>0\\ \text{then } D_L=\underset{D_L}{\text{Max}}\,\Omega\\ \\ \left(\dot{\xi}_1(t)-\dot{\xi}_2(t)\right)^2+\dfrac{\lambda_3}{A_{\infty 12}^2-\left(M_1+A_{\infty 11}\right)\left(M_2+A_{\infty 22}\right)}\times\\ \times\left(\left(M_2+A_{\infty 22}\right)\left(\dot{\xi}_2(t)-\dot{\xi}_1(t)\right)+A_{\infty 12}\left(\dot{\xi}_2(t)-\dot{\xi}_1(t)\right)\right)+\\ +\dfrac{\lambda_4}{A_{\infty 12}^2-\left(M_1+A_{\infty 11}\right)\left(M_2+A_{\infty 22}\right)}\times\\ \times\left(\left(M_1+A_{\infty 11}\right)\left(\dot{\xi}_1(t)-\dot{\xi}_2(t)\right)-A_{\infty 12}\left(\dot{\xi}_2(t)-\dot{\xi}_1(t)\right)\right)<0\\ \text{then } D_L=\underset{D_L}{\text{Min}}\,\Omega\end{cases} \tag{32}$$

If for some time intervals we get

$$\left(\dot{\xi}_1(t)-\dot{\xi}_2(t)\right)^2+\frac{\lambda_3}{A_{\infty 12}^2-\left(M_1+A_{\infty 11}\right)\left(M_2+A_{\infty 22}\right)}\times$$
$$\times\left(\left(M_2+A_{\infty 22}\right)\left(\dot{\xi}_2(t)-\dot{\xi}_1(t)\right)+A_{\infty 12}\left(\dot{\xi}_2(t)-\dot{\xi}_1(t)\right)\right)+$$
$$+\frac{\lambda_4}{A_{\infty 12}^2-\left(M_1+A_{\infty 11}\right)\left(M_2+A_{\infty 22}\right)}\times$$
$$\times\left(\left(M_1+A_{\infty 11}\right)\left(\dot{\xi}_1(t)-\dot{\xi}_2(t)\right)-A_{\infty 12}\left(\dot{\xi}_2(t)-\dot{\xi}_1(t)\right)\right)=0 \tag{33}$$

then singular arcs will be present in the solution. For these time intervals the control variable may take values between the maximum and minimum Ω-values. In such cases, the control variable will be made equal to a value implicitly given by the algorithm used to solve the problem.

To apply equation (32) it will be necessary to compute the adjoint variables over the time interval *T*. Applying the transversality equations and assuming the initial values for the state variables to be known but not $\xi_1(T)$, $\xi_2(T)$, $\dot{\xi}_1(T)$ and $\dot{\xi}_2(T)$ we find that $\lambda_1(T)=\lambda_2(T)=\lambda_3(T)=\lambda_4(T)=0$.

3 Numerical results

In order to illustrate the application of the stochastic and time-domain models, results were obtained for an axisymmetric two-body wave energy converter, represented in Fig. 1. It is assumed that body 1 is the body with a ring like shape (outside body). Body 2 is the inside body made of two parts (one surface-piercing body and a completely submerged cylinder) that oscillate together. For the stochastic model WAMIT© was used to compute the hydrodynamic diffraction and radiation coefficients for a set of 131 wave frequencies in the range of 0.05 rad/s to 1.2566 rad/s. For the time-domain model this range was extended to 2.5097 rad/s. The water depth is 50m.

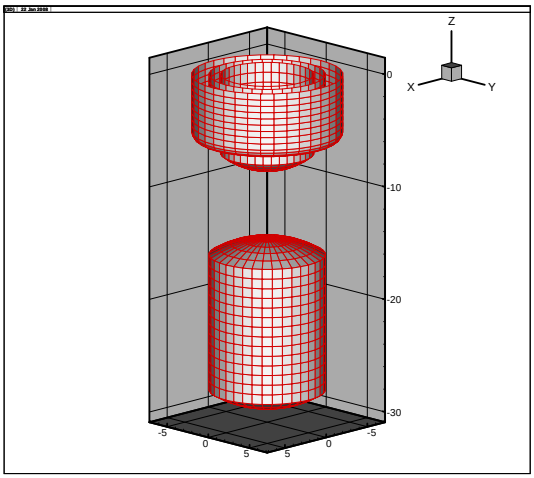

Figure 1: Panel grid describing the wet surface of the concentric axisymmetric oscillating bodies in numerical evaluation.

3.1 Stochastic model

Two scenarios were considered for the power take-off equipment: a) the PTO consists of a linear damper with a damping coefficient, D_L; b) the PTO consists of a linear spring, with stiffness K_L, and linear damper with coefficient D_L. The values of K_L and D_L that maximize the average useful power, and thus the capture width, λ_c, were computed. Results are obtained for the variance of ξ_1 and ξ_2, as well as for the variance of the load force, F_L. The optimized values of K_L and D_L for each sea state are also shown. To represent the sea states the following frequency spectrum was adopted ([10]):

$$S_\eta(\omega)=131.5H_s^2T_e^{-4}\omega^{-5}\exp\left(-1054T_e^{-4}\omega^{-4}\right) \tag{34}$$

The device behaviour was simulated for wave energy periods from 7 to 10s and significant wave height, H_s, equal to 2m. Figures 2 to 6 present, respectively, the capture width, mechanical damping coefficient, spring coefficient and variances for the displacement of both bodies, for the two mentioned power take-off scenarios. Figure 2 shows that the system has a better performance for sea states with smaller wave energy

period. This is more marked in the second power take-off scenario. For the considered range of wave energy periods the damping coefficient values obtained for scenario a) are greater than the ones obtained for scenario b) (Fig. 3). The spring coefficients computed for scenario b) may be negative or positive, depending on the wave energy period (Fig. 4). For scenario a) the curves for the displacement variance of both bodies present a very similar pattern (Fig. 5). This, however, does not happen for scenario b) (Fig. 6).

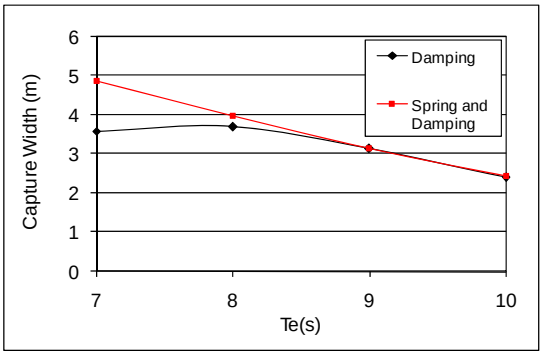

Figure 2: Capture width for wave energy periods from 7 to 10s and H_s equal to 2m, assuming that the power take-off equipment can be simulated by a damping coefficient D_L (black line) and assuming that the power take-off equipment can be simulated by both damping and spring coefficients D_L and K_L (red line).

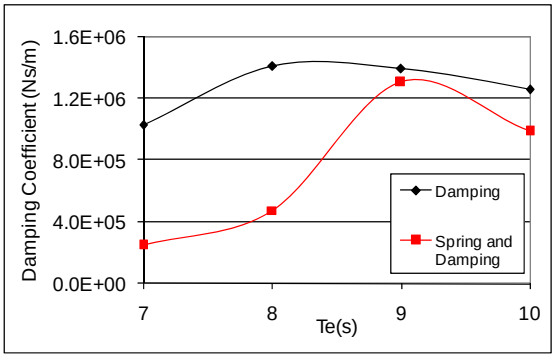

Figure 3: Mechanical damping coefficient for wave energy periods from 7 to 10s and H_s equal to 2m, assuming that the power take-off equipment can be simulated by a damping coefficient D_L (black line) and assuming that the power take-off equipment can be simulated by both damping and spring coefficients D_L and K_L (red line).

3.2 Time domain model

Since the memory effect in equations (14) and (15) is negligible after few tens of second, the infinite interval of integration in these equations may be, in practice, replaced by a finite one ([9]). For the purpose of this work a 60s interval was used. The values of the memory function defined by equation (16) and the

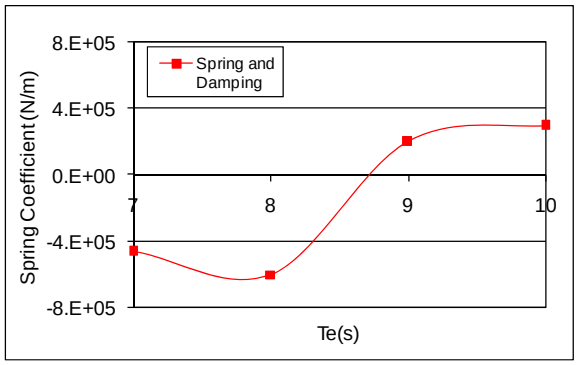

Figure 4: Mechanical spring coefficient for wave energy periods from 7 to 10s and H_s equal to 2m, assuming that the power take-off equipment can be simulated by both damping and spring coefficients D_L and K_L.

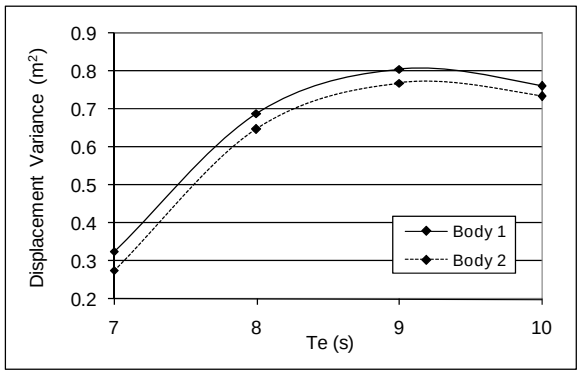

Figure 5: Variances for the displacements of body 1 and 2, for wave energy periods from 7 to 10s and H_s equal to 2m, assuming that the power take-off equipment can be simulated by a damping coefficient.

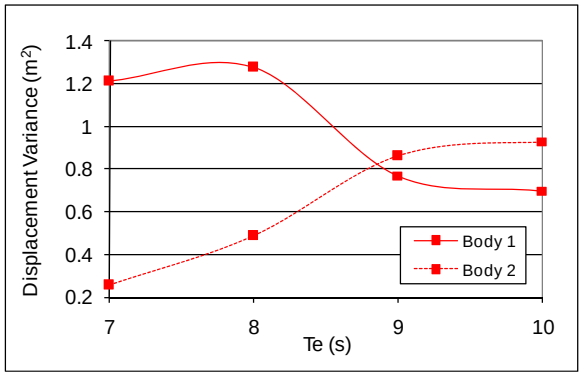

Figure 6: Variances for the displacements of body 1 and 2, for wave energy periods from 7 to 10s and H_s equal to 2m, assuming that the power take-off equipment can be simulated by both damping and spring coefficients D_L and K_L.

limiting values of the added mass, $A_{\infty_{ij}}$, were directly obtained from WAMIT©. Time series of 7200s, with a time step of 0.01s, were obtained for several values of the parameters that characterize the wave power device.

Time domain model (non-linear PTO)				
Npc	**G_m (m/Ns)**	**T (s)**	**$\bar{P}_U$ (kW)**	**Capture widht (m)**
1	9.00E-08	9.35	721.369	18.43
6	9.00E-08	9.35	720.385	18.40.
12	9.00E-08	9.35	709.777	18.13

Table 1: Average useful power and capture width results obtained from the time domain model for a 1m amplitude regular wave with a period of 9.35s, assuming different numbers for the pairs of cylinders.

In Table 1, the value of the flow proportionality constant G_m (see Eq. (18)) is the same for the three presented cases. Though the highest capture width value occurs for the case in which only one pair of cylinders is considered, it can be seen that the performance of the system is very similar for the three scenarios. Figures 7 to 9 present, for the case in which 6 pairs of cylinders are considered, the time variation of the displacements of body 1 and body 2, the relative displacement and velocity between the two bodies, and the useful power, for the interval $2740 \le t \le 2760$ s. It can be observed that, although body 1 and body 2 are practically never motionless (except for the instants when the direction of the motion changes - Fig. 7), sometimes the two bodies stay rigidly connected, i.e., the relative velocity between the two bodies is null, for some seconds (Fig. 8). When this occurs the production of energy clearly decays but never ceases (Fig. 9).

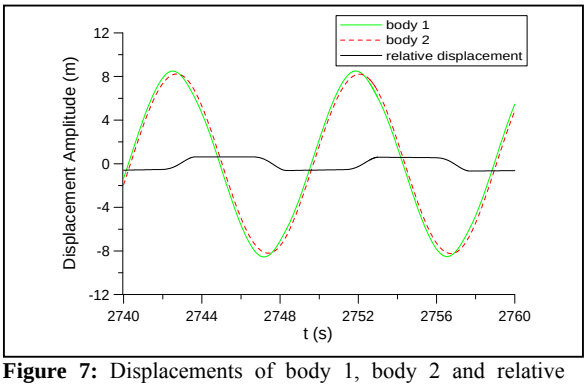

Figure 7: Displacements of body 1, body 2 and relative displacement between bodies for a 1m amplitude regular wave with a period of 9.35s, assuming a non-linear power take-off mechanism with 6 pairs of cylinders and $G_m = 9.00\text{E-}08$ m/Ns.

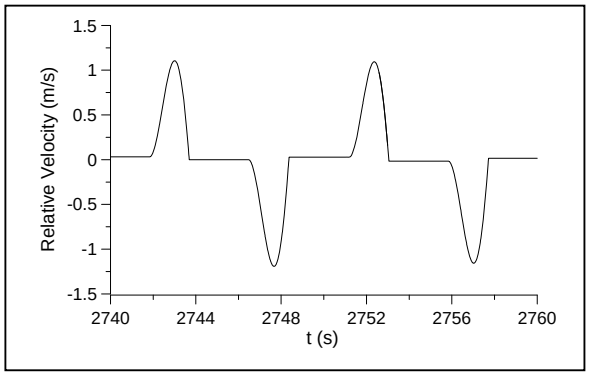

Figure 8: Relative velocity between body 1 and body 2 for a 1m amplitude regular wave with a period of 9.35s, assuming a non-linear power take-off mechanism with 6 pairs of cylinders and $G_m = 9.00\text{E-}08$ m/Ns.

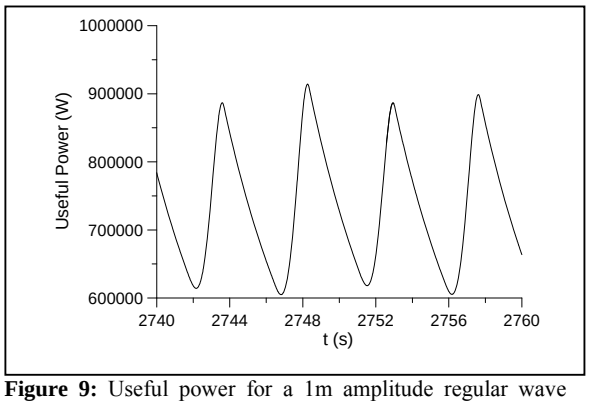

Figure 9: Useful power for a 1m amplitude regular wave with a period of 9.35s, assuming a non-linear power take-off mechanism with 6 pairs of cylinders and $G_m = 9.00\text{E-}08$ m/Ns.

To obtain the results for irregular waves the same spectral distribution defined by (34) was used. Figures 10 to 13 present, for the interval $2700 \le t \le 3000$ s, the time variation of the displacements of body 1 and body 2, the relative displacement and velocity between the two bodies, the useful power and the pressure inside both the high-pressure and low-pressure accumulators, as well as the pressure difference between the two accumulators, for significant wave height $H_s = 2$ m and wave energy period $T_e = 8$ s. A power take-off mechanism with 1 pair of cylinders and $G_m = 9.00\text{E-}08$ m/Ns was used. Again several time intervals can be observed in which, although the motion of body 1 and body 2 only ceases when it changes direction (Fig. 11), there is no relative motion between the bodies (Figs. 11 and 12). The production of energy drops accentually in these intervals (Fig. 12). From Fig. 13 it can be seen that this occurs when the pressure level inside the high-pressure accumulator also drops, which corresponds to a rising of the level inside the low-pressure accumulator. This remaining pressure difference when there is no relative motion between bodies keeps the flow of liquid through the hydraulic motor and thus the production of energy. The averaged capture width for this case was 3.0 m.

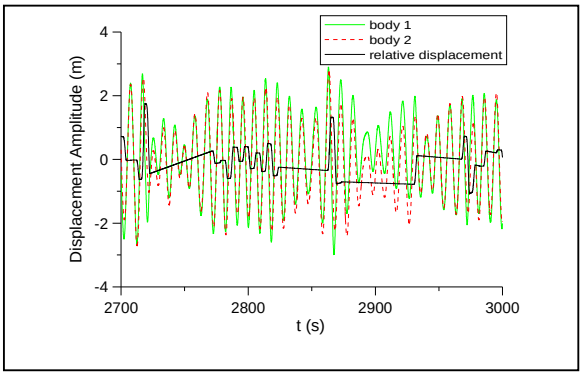

Figure 10: Displacements of body 1, body 2 and relative displacement between bodies for significant wave height $H_s = 2$ m and wave energy period $T_e = 8$ s, assuming a non-linear power take-off mechanism with 1 pair of cylinders and $G_m = 9.00\text{E-}08$ m/Ns.

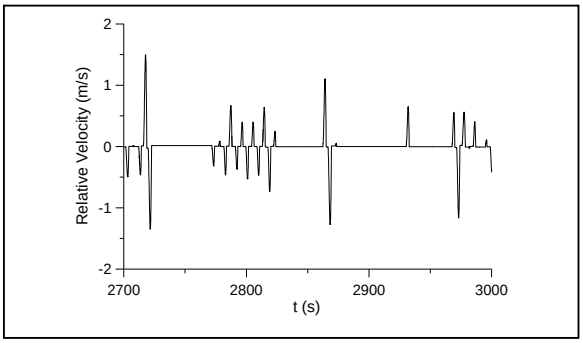

Figure 11: Relative velocity between body 1 and body 2 for significant wave height $H_s = 2$ m and wave energy period $T_e = 8$ s, assuming a non-linear power take-off mechanism with 1 pair of cylinders and $G_m = 9.00\text{E-}08$ m/Ns.

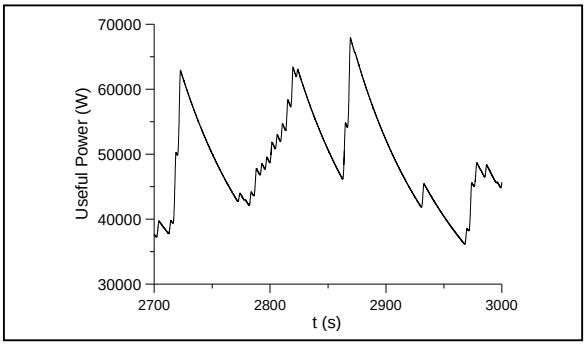

Figure 12: Useful power for significant wave height $H_s = 2$ m and wave energy period $T_e = 8$ s, assuming a non-linear power take-off mechanism with 1 pair of cylinders and $G_m = 9.00\text{E-}08$ m/Ns.

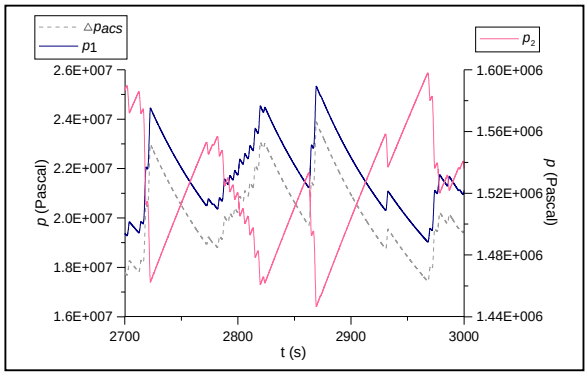

Figure 13: Pressure inside the high-pressure accumulator (p_1), inside the low-pressure accumulator (p_2) and pressure difference between the two accumulators (Δp_{acs}) for significant wave height $H_s = 2$ m and wave energy period $T_e = 8$ s, assuming a non-linear power take-off mechanism with 1 pair of cylinders and $G_m = 9.00\text{E-}08$ m/Ns.

Results for this same power take-off configuration were also obtained for significant wave height $H_s = 2$ m and energy periods equal to 7, 9 and 10s. Fig. 14 presents the comparison between these results (capture width) and the ones obtained from the stochastic model for the same H_s and T_e values. It can be seen that the patterns of the time-domain model curve and the stochastic model curve (particularly when assuming a power take-off system simulated by a damping) are identical: in both cases the highest capture width value occurs for $T_e = 8$ s and the smaller capture width values occur for the higher energy period values. The time-domain results were obtained for $G_m = 9.00\text{E-}08$ m/Ns and not for an optimized value of this parameter. This partially justifies the fact that the computed values are smaller than the ones obtained from the stochastic model. In order to achieve a better device performance, the optimization of this power take-off parameter is important. Figures 15 and 16 present the capture width values obtained for different G_m parameter values (only 1 pair of cylinders was considered) and different wave conditions. In Fig. 15 two curves are represented, corresponding to incident regular waves with amplitude of 1m and periods of 8 and 12s. For $T = 8$ s the highest capture width value (5.5m) is observed to $G_m = 1.00\text{E-}06$ m/Ns. For $T = 12$ s a larger G_m parameter value is required ($G_m = 1.00\text{E-}05$ m/Ns). The curve presented in Fig. 16 corresponds to irregular waves with $H_s = 2$ and $T_e = 12$s. In this case the highest capture width value (1.3m) occurs to $G_m = 5.00\text{E-}07$ m/Ns, representing a value 43% higher than the one obtained in the worst G_m scenario presented.

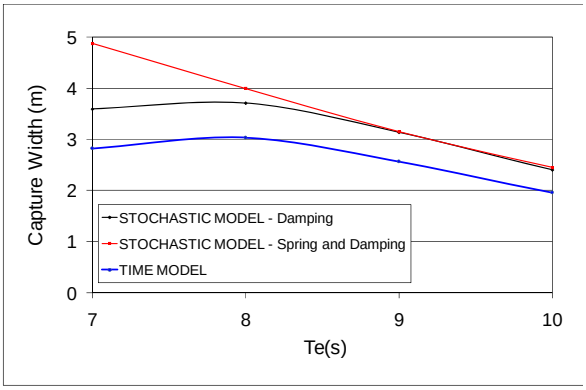

Figure 14: Capture width results for wave energy periods from 7 to 10s and H_s equal to 2m, obtained from the time domain model assuming a non-linear power take-off mechanism with 1 pair of cylinders and $G_m = 9.00\text{E-}08$ m/Ns (blue line) and obtained from the stochastic model, assuming that the power take-off equipment can be simulated by a damping coefficient D_L (black line) and assuming that the power take-off equipment can be simulated by both damping and spring coefficients D_L and K_L (red line).

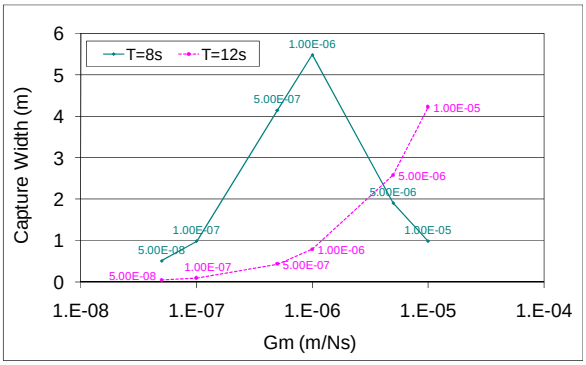

Figure 15: Capture width values obtained for different G_m parameter values (1 pair of cylinders is considered) and incident regular waves with amplitude of 1m and periods of 8 and 12s.

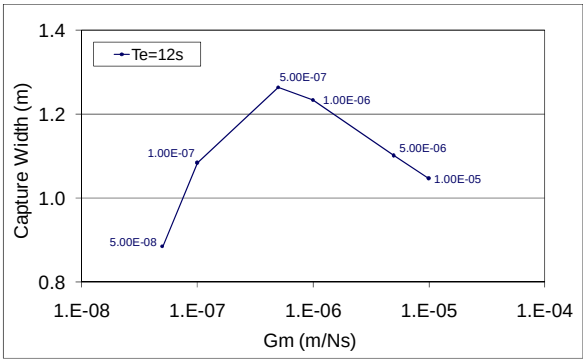

Figure 16: Capture width values obtained for different G_m parameter values (1 pair of cylinders is considered) and irregular waves with $H_s = 2\text{m}$ and $T_e = 12\text{s}$.

3.3 Pontryagin Maximum Principle

It was also assumed for the time domain model a load damping coefficient as described in section 2 (equations (22) and (23)). The use of PMP implies solving equations (30) backwards in time meaning that the knowledge in advance of the diffraction forces applied to the device during the time interval T is needed. The problem is non causal. In order to devise a control strategy, which may be considered causal, an approach based on PMP was devised. Thus, since PMP states that the optimum load damping coefficient should take the Ω maximum or minimum values (except for singular arcs), it is assumed that $D_L = \left\{ \underset{D_L}{\text{Min}}\,\Omega, \underset{D_L}{\text{Max}}\,\Omega \right\}$ for most of the time interval T. By setting a velocity limit for which D_L should change between $\underset{D_L}{\text{Min}}\,\Omega$ and $\underset{D_L}{\text{Max}}\,\Omega$ it will be possible to apply the control procedure to the device. However, note that this strategy will introduce large fluctuations in the power production, which may damage the energy quality from the electrical grid point of view (this problem might be mitigated by setting several devices in large array configurations). Indeed, this kind of fluctuations is characteristic of power take-off mechanism configurations with no energy storage system, such as the linear configuration here considered for the uncontrolled scenario.

Table 2 shows the amount of increased power production obtained with the considered control strategy. It should be noted that this is not an optimum control but instead it is based on the findings reached for PMP. Depending on the incident wave period there is a useful power increase of approximately 31% (test 1) and 41% (test 2). As expected, large P_u oscillations are observed, Fig. 17. For test 1 the minimum value for D_L is 6.76E4 Ns/m, when the relative velocity between bodies is lower than 0.55 m/s, and the maximum value is 10.14E5 Ns/m, when $\left|\dot{\xi}_1 - \dot{\xi}_2\right| > 0.6\text{m/s}$. For test 2, Fig. 18, the minimum value for D_L is 2.08E4 Ns/m and the maximum is 3.12E5 Ns/m, respectively when $\left|\dot{\xi}_1 - \dot{\xi}_2\right| < 0.2\text{m/s}$ and $\left|\dot{\xi}_1 - \dot{\xi}_2\right| > 0.25\text{m/s}$.

4 Conclusions

Stochastic and time-domain models were developed for an articulated device composed by two coaxial bodies. The use of the stochastic model for irregular waves allows finding variances that define Gaussian probability density functions for relevant wave device parameters. It was assumed that the power take-off mechanical equipment has a linear behaviour and can be modelled by spring and damping coefficients. Its characteristics were assumed to be constant for the duration of a sea state. For the time-domain model a

Time domain model (linear PTO)			
Test	**D_L (Ns/m)**	**T (s)**	**$\bar{P}_u$ (kW)**
Uncontrolled	Best D_L 6.76E5	8.02s	125.7
1	Min=6.76E4 Max=10.14E5	8.02s	164.7
Uncontrolled	Best D_L 2.084E5	10.05s	93
2	Min=2.084E4 Max=3.12E5	10.05s	130.8

Table 2: Average useful power results obtained from the time domain model for a 1m amplitude regular wave, for the uncontrolled and controlled device.

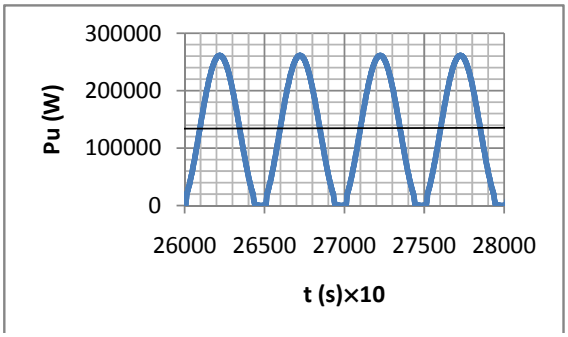

Figure 17: Useful power values obtained for test 2, T=10.05s and 1m wave amplitude.

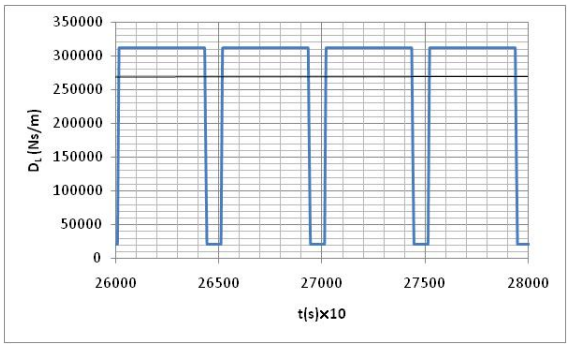

Figure 18: D_L values obtained for test 2, T=10.05s and 1m wave amplitude.

non-linear power take-off mechanism configuration was devised. Results were obtained for regular and irregular waves. The results for irregular waves were compared to the ones computed by the stochastic model and a good agreement was found between them. The capture width values for the stochastic model and for the time-domain model, assuming a non-linear power take-off mechanism, obtained in irregular waves conditions are significantly lower than the ones obtained for regular waves. The articulated device performance proved to be highly sensitive to the characteristic parameters of the non-linear power take-off mechanism. In order to obtain a better performance, further optimization of these parameters and device control are essential. Pontryagin Maximum Principle was analytically developed as an algorithm for the control of the device, considering the power take-off mechanism simulated by a damping term. An empirical algorithm based on PMP was tested for incident regular waves, increasing the useful power.

References

[1] M. E. McCormick. Ocean wave conversion. *A Wiley-Interscience Publication*, John Wiley & Sons, 1981.

[2] M.A. Srokosz and D.V. Evans. A theory for wave-power absorption by two independently oscillating bodies. *J. Fluid Mechanics*, 90(2):337-362, 1979.

[3] A. Clément, A. Babarit, J-C. Gilloteaux, C. Josset and G. Duclos. The *SEAREV* wave energy converter. In *Proc. 6th European Wave and Tidal Energy Conference*, Glasgow, 2005.

[4] P.A.P. Justino and A. Clément. Hydrodynamic performance for small arrays of submerged spheres. In *Proc. 5th European Wave Energy Conference*, Cork, 2003.

[5] S. Mavrakos. Hydrodynamic coefficients in heave of two concentric surface-piercing truncated circular cylinders. *Applied Ocean Research*, 26:84-97, 2004.

[6] A.F. de O. Falcão and R.J.A. Rodrigues. Stochastic modelling of OWC wave power plant performance. *Applied Ocean Research*, 24:59-71, 2002.

[7] L.M.C. Gato, P.A.P. Justino and A.F. de O. Falcão. Optimization of power take-off equipment for an oscillating-water column wave energy plant. *6th European Wave and Tidal Energy Conference*, Glasgow, 2005.

[8] M.T. Pontes, J. Cândido, J.C.C. Henriques and P. Justino. Optimizing OWC sitting in the nearshore. In *Proc. 6th European Wave and Tidal Energy Conference*, Glasgow, 2005.

[9] A.F. de O. Falcão. Modelling and control of oscillating-body wave energy converters with hydraulic power take-off and gas accumulator. *Ocean Engineering*, 34:2021-2032, 2007.

[10] Y. Goda. *Random Seas and Design of Maritime Structures.* University of Tokyo Press 1985.